International Journal of QUANTUM CHEMISTRY

Functional Molecules and Materials by π-Interaction Based Quantum Theoretical Design

Zahra Aliakbar Tehrani* and Kwang S. Kim*

The intermolecular and intramolecular noncovalent interactions involving π-aromatic compounds have attracted increasing attention over the last decades in chemistry, biology and material sciences. In this review, we discuss contemporary computational studies on the nature and strength of H-π, π-π, and anion-π interactions. We emphasize how modern quantum theoretical approaches ahead of experiment can provide insight into the design of new materials and devices by tuning the π-interactions in cooperative and competitive manners. Usefulness of such approaches towards designing new materials is demonstrated with some examples of molecular recognition/sensing, self-assembly/engineering, receptors, catalysts, supramolecules, graphene, and other two-dimensional (2D) materials/devices. © 2016 Wiley Periodicals, Inc.

DOI: 10.1002/qua.25109

Introduction

Interactions between molecules are generally represented by electrostatic interaction, polarization, dispersion interaction, and exchange repulsion. Molecular interactions could be categorized based on the type of bonding involved: covalent and noncovalent. Noncovalent interactions[1] differ from covalent bonding as the former relies on electrostatic interactions instead of electron sharing. They can be classified into various types of interaction such as hydrogen bonding, halogen bonding, π-interactions, and ionic interactions. Noncovalent interactions are critical factors for controlling structural and energetic aspects of molecular recognition/sensing and self-assembling/engineering.[2–4] π-Systems can noncovalently bind to diverse molecular systems. Various types of π-interactions include H-π,[5,6] π-π,[7–9] π^+-π,[10] π^+-π^+,[11] cation-π,[7,12–14] π^--π, π^--π^-,[15] and anion-π[16–21] interactions (Fig. 1). Over the past decades, π-interactions have been extensively studied due to their application in protein-complexes, receptors, supramolecular chemistry, crystal packing, nanomaterials, and electronic/spintronic devices.[22–25]

Accurate analysis of intermolecular interactions with high level theoretical methods helps design of new functional molecules and materials with desired physical and chemical properties. The computational chemistry as a guiding tool toward designing materials and devices with unique properties has recently attracted great interest.

In the first section of this review, given that cation-π interactions are rather well discussed in a few review papers,[7,12–14] we briefly discuss about the fundamental aspects and the factors influencing nature and strength of H-π, π-π, and anion-π interactions. These interactions play important roles in diverse fields of chemistry, biology and material sciences. We show how interaction energy decomposition analysis with symmetry-adapted perturbation theory (SAPT) provides insight into the nature of noncovalent interactions. In the second section, we illustrate some representative examples related to molecular recognition/sensing, self-assembly/engineering, nanomaterials/devices, and catalysts by tuning these intramolecular interactions in cooperative and competitive ways.

Factors Influencing π Interaction Strengths

H-π and π-π interactions

The H-π and π-π (π stacking) interactions are termed as attractive noncovalent interactions of the π electronic cloud of an aromatic compound with the positively charged H moiety (in –CH, –NH, etc) and the π electronic cloud of another aromatic compound, respectively. The benzene dimer (T-shaped edge-to-face, parallel-displaced, and eclipsed face-to-face; Fig. 2) as simple H-π and π-π interaction models with small binding energy (~1.5–3 kcal/mol) has received a great attention from both experiment and theory over last decades.[8,26–30]

The binding energy of the benzene dimer at the coupled cluster with single, double and perturbative triple excitations level [CCSD(T)] using the complete basis set (CBS) limit shows that the T-shaped edge-to-face conformer is nearly isoenergetic (~2.5 kcal/mol in zero-point-energy corrected binding energy) to the parallel-displaced face-to-face conformer.[8] The strength and configurational orientation of H-π and π-π interactions can be controlled by replacing H or C atoms (heteroatom effect) with other atoms or chemical groups. For example, in the $C_6F_6\cdots C_6H_6$ dimer the most favorable conformer is the parallel-displaced ($\Delta E = -5.38$ kcal/mol at the CCSD(T) level) followed by the face-to-face and T-shaped geometries.[31] According to the Hunter-Sanders rules[32] (HS hypothesis), the π electron density cloud of aromatic ring changes according to the electronic character (electron-donating/withdrawing) of the substituent. Therefore, the substituent effect as nonlocal

Z. A. Tehrani, K. S. Kim
Department of Chemistry, Ulsan National Institute of Science and Technology (UNIST), Ulsan, 689-798, Korea Fax: (+82) 54 279 8137 E-mail: zahratehrani7@yahoo.com or kimks@unist.ac.kr

Z. A. Tehrani received her Ph.D. degree in physical organic chemistry from Sharif Univ. of Tech. After 2 years postdoctoral experience in Chemistry and Chemical Engineering Research Center of Iran, she is a postdoctoral fellow at Ulsan National Institute of Science and Technology (UNIST). Her research interests include reaction mechanism of organic/biological systems and noncovalent interactions in materials.

K. S. Kim received his Ph.D. degree from University of California, Berkeley. He was a professor in POSTECH. Currently, he is a distinguished professor in Department of Chemistry and the Director of the Center for Superfunctional Materials at UNIST. His research interests include theoretical design and experimental development of novel functional molecular/material systems and nano devices.

and indirect effect adds or withdraws electron density inductively from the π system. Consequently, the electrostatic effect is the dominant factor in stability of π-stacked dimers of mono-substituted benzene. Correlation of substituent effects on the stability of π-π stacking interactions is also investigated with computed electrostatic potentials (ESPs) and Hammett σ-constants models.[8,27,33–35] These models reveal that electron-withdrawing substituents enhance stacking interactions in benzene dimers while electron donating substituents give the opposite effect and hinder stacking interactions.

Tarakeshwar et al. studied the H-π interaction using the systems of an olefinic (ethene)/aromatic (benzene) π compound interacting with one of HX (X: halide), H_2O, NH_3, and CH_4 molecules.[6] The electron withdrawing/donating substituents on the para-position of the edge molecule of the T-shaped benzene dimer destabilize/stabilize the benzene dimer, where the Hammett constant σ_p is highly correlated with the binding energy.[27] The electrostatic interaction due to substitution (though smaller than dispersion) governs the change of the binding energy, because the exchange-repulsion and dispersion terms tend to be almost cancelled.[27] On the other hand, the substituents on the face molecule were not correlated with the Hammett constant.

Sinnokrot and Sherrill reported that a few substituents including electron-donating and electron-withdrawing groups stabilized stacked benzene dimers.[36] This was further confirmed for many other stacking conformers for diverse substituents regardless of electron donating or withdrawing nature by Lee et al.[8] For halogen substituted benzene sandwich dimer, Clements and Lewis[37] reported that stacking interaction energies based on Møller-Plesset second-order perturbation theory (MP2) are correlated to Hammett constants σ_p, while there is no correlation between the quadrupole moments of the halogenated ring with interaction energies. Wheeler and Houk[38] reported the stacking energies of 25 mono-substituted benzene sandwich dimers, where all types of substituents stabilized the benzene sandwich dimer. It indicated that electrostatic effects determine the stability of dimers, while dispersion interactions cause just a relatively constant shift for all substituted dimers. This trend was also confirmed by linear correlation (Fig. 3) between Hammett σ_m constant and interaction energies in substituted dimers. They also discovered that substituent effects in sandwich dimers are the same as in the $HX\cdots C_6H_6$ model.[38]

The interaction energies and additivity of substituent effects in the parallel-displaced benzene dimers are found to be similar to those in the sandwich dimers. Consequently, most of reported findings in sandwich dimers would be applicable in parallel-displaced ones.[39,40]

The benzene and perfluorobenzene have quadrupole moments with same magnitude and opposite sign.[41] Therefore, perfluorinated π-π dimers should have different characters compared with the nonfluorinated case as found experimentally.[41] The quadrupole stacking between aromatic and perfluoroaromatic rings allows specific protein–protein

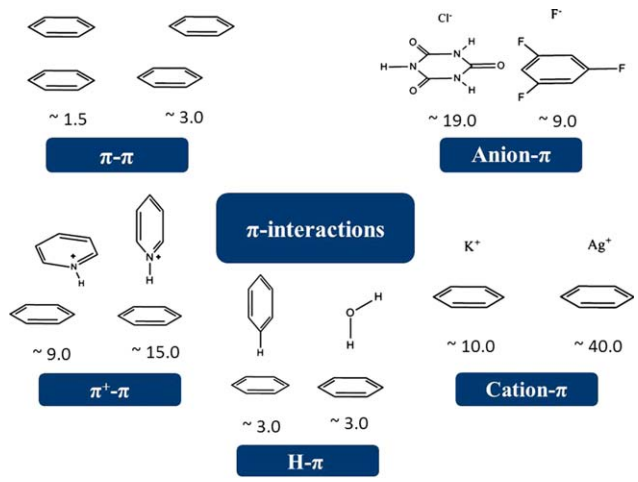

Figure 1. Various types of π-interactions (the typical binding energies are given in kcal/mol). Reproduced from Ref. [10], with permission from American Chemical Society.

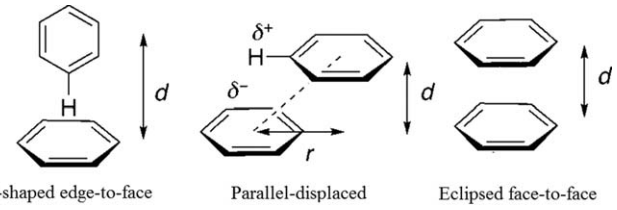

Figure 2. Representative conformations of the benzene dimer.

interactions and de novo peptide design.[42] Zheng and Gao[43] reported quadrupole interaction as a new tool for peptide-peptide molecular recognition. The electron-donating substituents stabilized the π-π interaction in both sandwich and parallel-displaced $C_6F_6\cdots C_6H_5X$ dimers.[38] Comprehensive study on 25 substituted benzene–perfluoro-benzene sandwich dimers revealed that resonance effects play a key role in stabilizing perfluoro dimers (Fig. 3). Furthermore, these dimers showed opposite substituent effects compared with benzene sandwich dimers. Wheeler reported[40] the results based on dispersion corrected density functional theory (DFT-D; B97-D) and CCSD(T) for a series of sandwich dimers of the substituted $C_6F_6\cdots C_6H_5X$ and for the substituted benzenes interacting with 1,2,3-trifluorobenzene by using the local and direct interaction models. These new models represent *additivity* and *transferability* of substituent effects in stacking interactions. Based on these findings individual or local interacting models would be applicable for investigation of the substituent effect in complex aromatic systems.

SAPT analysis

Accurate descriptions of the physical origin of noncovalent interactions are important in designing new materials and molecules having desired properties. SAPT analysis[44] with various approaches (such as SAPT0, SAPT2, DFT-SAPT, etc.)[45,46] properly describes intermolecular interactions in conjunction with high-level *ab initio* methods in molecules, functional groups, and fragments. In the SAPT theory, the total interaction energy of systems is decomposed into electrostatic (E_{es}, including charge-charge, charge-dipole, and dipole-dipole interactions), induction (E_{ind}, including dipole/induced-dipole interactions), dispersion (E_{disp}), and exchange-repulsion (E_{exch}) components [or effective induction (E_{in}), effective dispersion (E_{dp}), and effective exchange-repulsion (E_x) components].[7,8,44]

The nature and strength of π interactions are governed by competition among electrostatic, inductive and dispersive attractive, and exchange repulsive interactions of the π system with counter molecules (such as cation, anion, π, and –CH/NH).[10] Cation-π interactions have large electrostatic and induction energies and somewhat small dispersion energy, while non-metallic cation-π interactions (such as ammonium and alkyl ammoniums) have large electrostatic and dispersion contributions and substantial induction energy.[10] In the anion-π interaction, the exchange-repulsion energy component increases (as a result of repulsion between the electron densities of π systems and an anion) as compared with cation-π systems. In π-π systems with similar electron densities (face-to-face sandwich benzene dimer) the dispersion energy component is dominant, whereas induction energy and charge transfer are key factors in the interaction of electron-deficient/electron-rich π-π systems (hexafluoro-benzene-benzene dimer).[10]

The intermolecular distance (short-range, midrange, and long-range distances as compared with the optimal energy distance) and interaction energy of the displaced-parallel benzene dimer are affected by dispersion corrections. For example, SAPT results of displaced-parallel benzene dimer at PBE0AC/aVTZ are close to CCSD(T)/CBS. Density functional theory (DFT) including dispersion interactions such as dispersion-corrected DFT (DFT-D)[47] [including Grimme's D3,[48] Tkatchenko−Scheffler's (TS),[49] and Becke-Johnson's (BJ)[50] which can be combined with a variety of density functionals] and nonlocal correlation methods (van der Waals density functional such as vdW-DF2),[51] slightly overestimate the interaction energies, but the overall magnitude is acceptable. Therefore, DFT-D methods are useful for understanding the properties of π interactions of moderate size systems which cannot be dealt with accurate *ab initio* calculations.[52] Indeed, they have shown remarkable success in computer aided molecular design of π systems. An overview of computational methods suitable to the study of noncovalent π interactions was reported by Riley et al.[53]

Sinnokrot and Sherrill provided helpful insights to substituent effects in π-π interactions. SAPT results[54] for monosubstituted sandwich benzene dimers (with OH, CH_3, F, and CN substituents) in Figure 4 shows: (i) for CN and F withdrawing substituents, the electrostatic energy component is much more favorable than the others, and (ii) for CH_3 and OH donating substituents the dispersion and exchange components have larger contributions to the relative total energy. They also used F-SAPT (functional-group partition of SAPT), ESP, and density analyses for investigating influence of substituents on π-stacking interactions in both Hunter-Sanders (HS) and Wheeler-Houk (WH) pictures.[55] As for the total substituent effect, the exchange, electrostatic and induction terms are

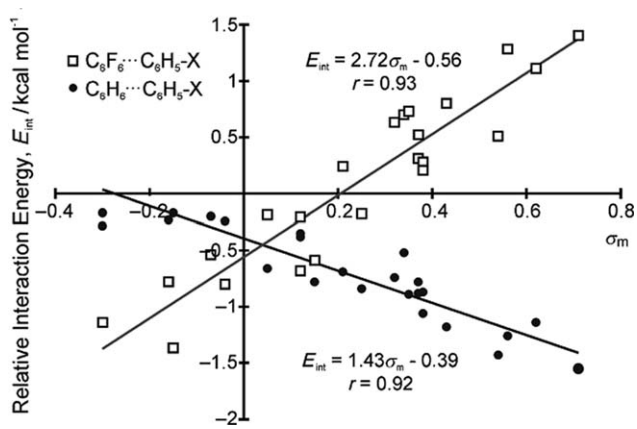

Figure 3. Interaction energies for sandwich dimers of 25 monosubstituted benzenes versus Hammett σ_m constants for benzene (•) and perfluorobenzene (□) calculated at M05-2X/6-31 + G(d) level. Reproduced from Ref. [38], with permission from American Chemical Society.

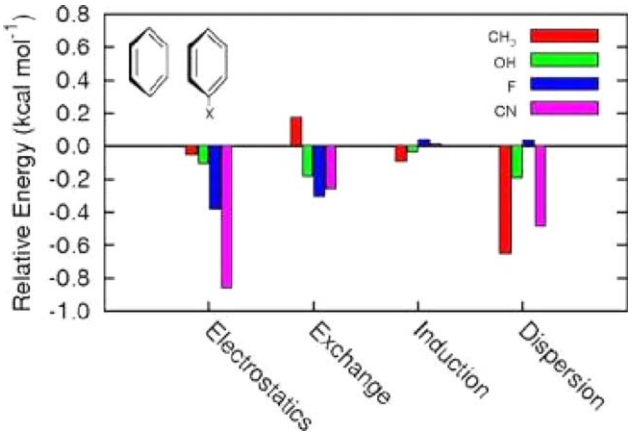

Figure 4. Interaction energy components relative to the benzene dimer for monosubstituted sandwich benzene dimers calculated at SAPT2/jun-cc-pVDZ level. Reproduced from Ref. [54], with permission from American Chemical Society.

important in the HS picture, while the electrostatic and dispersion terms are important in the WH picture. The SAPT2 energy component analysis of pyridine dimers[56] (Table 1) revealed that the dipole-dipole electrostatic interactions stabilized anti-aligned pyridine dimer (−3.05 kcal/mol, $\delta E_{elst} = -1.29$ kcal/mol) more than the pyridine aligned dimer (−1.69 kcal/mol, $\delta E_{elst} = -0.05$ kcal/mol). The smaller polarizability of pyridine than benzene makes the dispersion component unfavorable in the pyridine dimer than the benzene dimer.

Ab initio investigation on π dimers of N-heterocycles (pyridine (Py), pyrazine (Pz), triazine (Tz), and tetrazine (Tt) in stacked (S), displaced-stacked (D), and T-shaped series (T)) using the Cambridge Structural Database showed stacked/displaced-stacked preference in their conformations.[57] Although the dispersion effect is dominating in stacked/displaced-stacked dimers, their relative stabilities are controlled by electrostatic effects (Fig. 5).

Anion-π interaction

During the past decades, the anion-π interaction has been widely investigated in both theoretical and experimental domains due to its structural and functional significance.[16–21,58] The anion-π interaction is termed as attractive noncovalent interaction between an electron deficient or π-acidic aromatic system and an anion. An anion can interact with a π system through hydrogen bonding, noncovalent anion-π interactions and covalent σ interactions.[59] For instance, chloride and azide anions interact with π system of s-triazine and trifluorotriazine molecules (anion-π interaction) while fluoride forms a covalent bond with an aryl carbon of these molecules (via covalent σ interaction).[16] Interaction of simple anions with π electronic cloud of aromatics is enthalpically less favorable than that with aryl hydrogens.[60] Interaction mode of an anion with a given π system depends on the nature of anion. For example, nucleophilic anions such as F^-, CN^-, and OR^- interact with electron-deficient arenes via covalent σ interaction, while charge-diffuse anions such as ClO_4^-, BF_4^-, and PF_6^- form anion-π complex with these arenes.[61] The directional character of anion-π systems has clearly been revealed from the Cambridge Structural Database.[20] Anions tend to be located above the ring but not exactly over the ring centroid.

Table 1. SAPT energy component analysis (in kcal/mol obtained at SAPT2/jun-cc-pVDZ level with separation distance of 3.8 Å) of benzene-benzene $(Bz)_2$, benzene-pyridine (Bz-Py), and pyridine-pyridine $(Py)_2$ dimers.

	E_{elst}[a]	E_{ind}	E_{exch}	E_{disp}	$E_{exch}+E_{disp}$[b]	SAPT2
$(Bz)_2$	−0.48	−0.28	4.52	−5.68	−1.17	−1.92
Bz-Py	−0.80	−0.26	4.00	−5.34	−1.34	−2.39
$(Py)_2$ aligned	−0.05	−0.21	3.57	−5.00	−1.44	−1.69
$(Py)_2$ antialignd	−1.29	−0.25	3.49	−5.00	−1.51	−3.05

Adapted from Ref. [56]. [a] In kcal/mol; obtained at SAPT2/jun-cc-pVDZ level with separation distance of 3.8 Å. [b] The sum of the exchange and dispersion components.

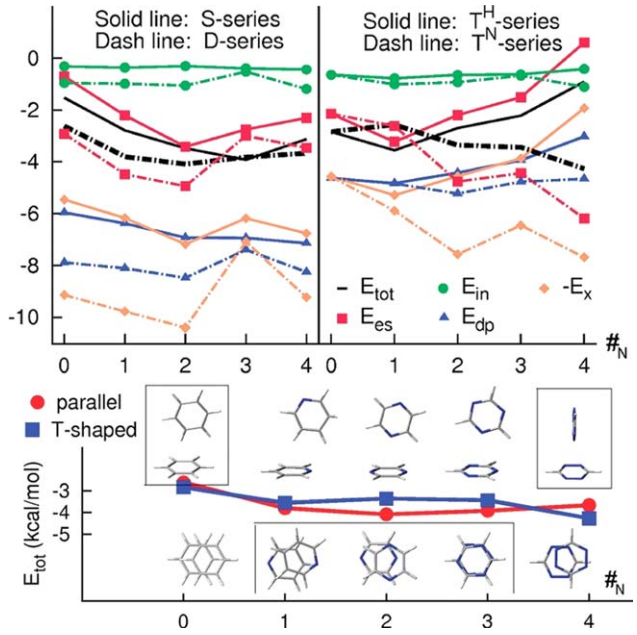

Figure 5. Interaction binding energies and energy components as a function of the number of N atoms (#N) in a series of π dimers of N-heterocycles. Lowest energy dimers are enclosed in boxes. Reproduced from Ref. [57], with permission from American Chemical Society.

The anion-π complexes have significant induction, electrostatic, and dispersion energy.[18,19,58] In particular, the ion-induced polarization and electrostatic terms are the main contributors to the anion-π interaction.[62] The electrostatic and polarization terms are associated with quadrupole moment (Q_{zz}) and molecular polarizability ($\alpha_{||}$) of the π systems, respectively. The induction component arises from interaction of p/π orbital of anions (halides or organic anions) with the LUMO of the aromatic systems. The interaction energies of anion-π systems are somewhat smaller than hydrogen bonding but comparable to those of cation-π systems ($E_b = 18.4$ kcal/mol for $C_6F_6\cdots F^-$ complex[19] *versus* $E_b = 22.3$ kcal/mol for $C_6H_6\cdots Na^+$ complex[10] calculated at the MP2/aug-cc-pVDZ level). The strength of single anion-π interaction varies widely (−3.6 kcal/

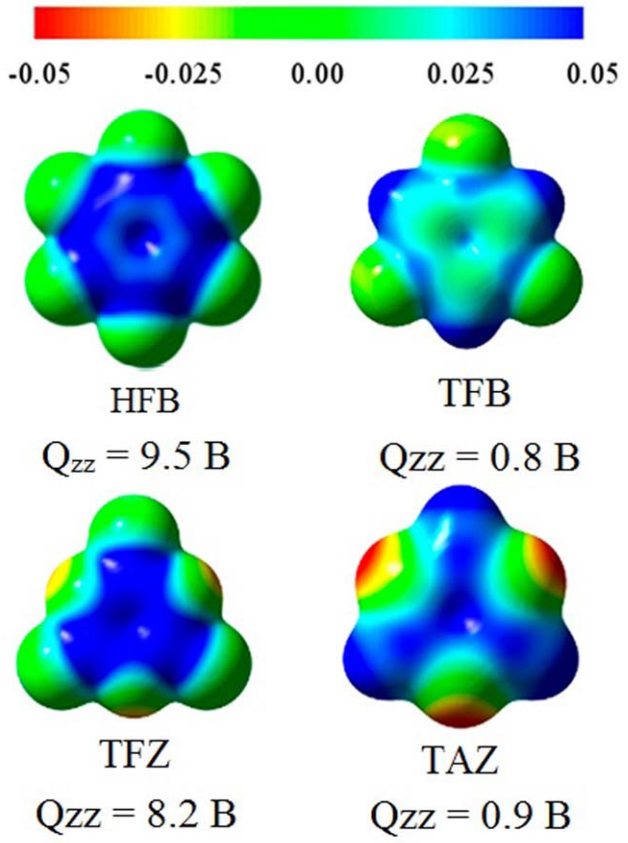

Figure 6. Electrostatic potential surfaces of hexafluorobenzene (HFB), 1,3,5-trifluoro-benzene (TFB), 2,4,6-trifluoro-1,3,5-triazine (TFZ), and 1,3,5-triazine (TAZ) (at PBE/ATZ level with electron isodensity value of 0.005 a.u). Reproduced from Ref. [70], with permission from American Chemical Society.

mol in 1,4-difluorobenzene$\cdots Cl^-$ system to −32.7 kcal/mol in cyameluric acid($C_6N_7O_3H_3$)$\cdots Cl^-$ system,[63] and −86.1 kcal/mol in the heptazine derivative $C_3N_7(CN)_3\cdots F^-$ system[64]).

To tune anion-π interactions, the π system should have large molecular polarizability ($\alpha_{||}$) and quadrupole moment (Q_{zz}).[65,66] The quadrupole moment of π system can be enlarged by introducing strong electron-withdrawing groups (such as $-NO_2$, CN, and –F groups), while the polarizability can be tuned by the size increase of the aromatics (large polycyclic aromatic conjugated systems such as naphthalene, pentacene, and coronene). For example, as a result of replacing H-atoms in benzene by fluoro groups in hexafluoro-benzene, the Q_{zz} reverses the sign ($Q_{zz} = -8.7 \pm 0.5$ in benzene to $Q_{zz} = +9.50$ B in hexafluoro-benzene) and the anion-π interaction becomes attractive from the unfavorable situation for benzene.[65] However, Wheeler and Houk presented that the interactions between arene and anion could not be described by quadrupole moment as quantitative predictor.[67] It is because attractive interaction between anion and the local dipole associated with the substituent in arene makes anion-π complexes energetically favorable.

It is worth mentioning that the electrostatic term of anion-π interaction can also be described in terms of ESP as the quantitative predictor of anion-binding energies which are widely used to characterize π-acidity of aromatics and heterocycles.[68,69] For example, ESP maps (Fig. 6) for 1,3,5-trifluorobenzene (TFB), hexafluorobenzene (HFB), 2,4,6-trifluoro-1,3,5-triazine (TFZ), and 1,3,5-triazine (TAZ) molecules demonstrate that the TFZ surface has a higher positive potential above the center of aromatic ring compared with other molecules. Therefore, it can be used as good candidate for detecting anions via anion$-\pi$ interactions.[70] The CCSD(T)/CBS binding energies of TFB (−10.86 kcal/mol), HFB (−21.08 kcal/mol), TZF (−27.67 kcal/mol), and TAZ (−11.90 kcal/mol) ligands to an F^- anion confirm the potential application of TFZ and HFB as selective recognition of F^-.[70] Selective anion recognition can be achieved with optimal geometry and charge distribution of anion-π systems.[64]

Kim et al. reported that electrostatic and induction effects control the stability of nitrate and chloride complexes with hexafluoro-benzene and triazine.[19] Their SAPT(MP2)/aVDZ′ results for various complexes of halides with benzene and trisubstituted benzene systems showed that the induction effect plays an important role as the net stabilization parameter in these complexes.[71] Mezei et al. used electrostatic potential maps and SAPT energy decomposition analysis (SAPT0/jun-cc-pVDZ) for explanation of the origin of anion-π interactions in diverse complexes listed in Figure 7.[70] Based on their SAPT results, the repulsive exchange, attractive electrostatic, induction, and dispersion energy components are on average composed of −131%, 122%, 60%, and 50% of the total interaction energy, respectively. The exchange and electrostatic terms are larger in the complexes that the centers of anion and aromatic ring with larger quadrupole moment are close together. The induction and vdW dispersion energies are important in the Br^-/CO_3^- complexes with aromatics rings with small quadrupole moments.[64]

Columbic repulsion between anions and aromatics with negative quadrupole moment makes anion-π interactions unstable. However, the electrostatic repulsion term in these complexes (based on SAPT(MP2)/aVDZ′ results) can be overcome by induction effects arising from the alkyl substitution on aromatics.[71] Results obtained at CCSD(T)/CBS limit for electron-rich alkyl/alkenyl/alkynyl-substituted benzenes and triphenylene systems confirmed the correlation of the system stability with chain length, unsaturation, and halogenation in aromatics. Comparison of $BzEt_3\cdots F^-$, $Bz(CHCH_2)_3\cdots F^-$, and $Bz(CCH)_3\cdots F^-$ binding energies, from −0.86 kcal/mol in

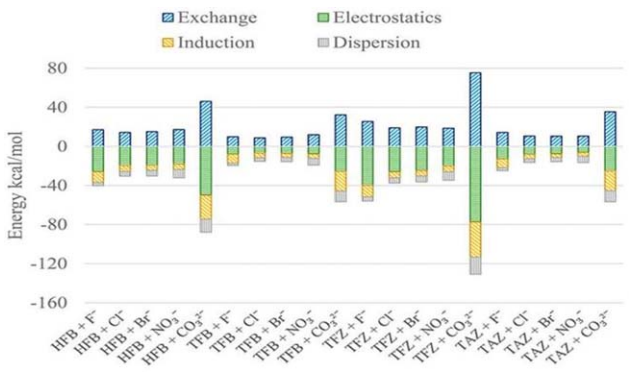

Figure 7. SAPT0/jun-cc-pVDZ energy component analysis of the interaction energy of some anion$-\pi$ binary complexes. Reproduced from Ref. [70], with permission from American Chemical Society.

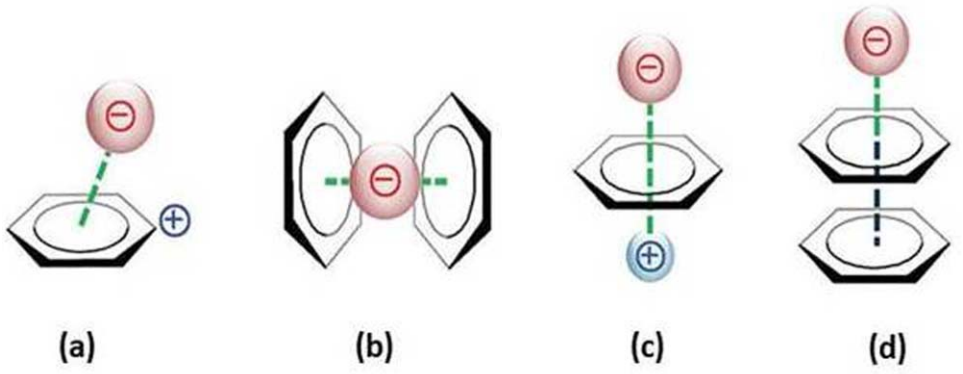

Figure 8. Illustration of the different anion-π interaction enhancement factors: a) positive charge on the π system, b) additivity of the anion-π interaction, c) cation–π-anion interaction, and d) π-π cooperative effects. Adapted from Ref. [21], with permission from The Royal Society of Chemistry.

$BzEt_3\cdots F^-$ to -7.11 kcal/mol in $Bz(CCH)_3\cdots F$, demonstrate the dramatic effect of unsaturation in stability of systems.[71] Moreover, halogenation of substituents increases stability of investigated systems: $Bz/BzF_3\cdots F^-$ (0.66/-9.31 kcal/mol), $BzMe_3/Bz(CH_2F)_3\cdots F^-$ ($-0.38/-14.55$ kcal/mol), and $Bz(CCH)_3/Bz(CCF)_3\cdots F^-$ ($-7.11/-9.29$ kcal/mol).[71]

Other alternative ways to strengthen the anion-π interaction (Fig. 8) are to introduce (a) a positive charge on the π system (increasing interaction energy up to -94.4 kcal/mol for tropylium cation-fluoride system at the RI-MP2/6-31++G** level),[72] (b) additivity of the anion-π interaction,[73] (c) cation–π-anion interaction[74,75] and (d) π-π cooperative effect[76] or π-π -anion interactions. For example, stacking of hexafluorobenzene with the π electronic cloud of the benzene ring in the benzene-F^- complex stabilizes the complex by changing its binding energy from $+2.8$ kcal/mol to -6.5 kcal/mol.[76] The additivity of anion-π interaction is well demonstrated in complexes between Cl^-/Br^- anions and s-triazine. Accordingly, the binding energies of Br^- anion to s-triazines, binary and ternary sandwich complexes are -5.0, -10.2, and -21.7 kcal/mol, respectively.[73]

Insight to material design

In this section, we highlight some of recently published theoretical and/or experimental studies that illustrate rational design of new materials by tuning the strength and type of H-π, π-π, and anion-π interactions.

Molecular recognition and sensing

Molecular recognition refers to the specific interaction between the host and its specific guest molecules via noncovalent interactions. Understanding the structural features of receptor and guest, as well as the nature of their interaction, is necessary for designing suitable receptors which have high selectivity to their guest.[2,4]

Morphological transformation of self-assembly structures (organic molecules) is guided by tuning intramolecular noncovalent interactions. Shape-engineering control of calix-[4] hydroquinone (CHQ)[77] as a result of changing temperature, diffusion and evaporation rates (which can highly control the strength and direction of π-π stacking and H-binding interactions of CHQ), provides nanotube, nano sphere as well as nanolens structures.[77,78]

Recognition of fullerene C_{60} is challenging, which requires the control of weak π-π, van der Waals, and charge-transfer interactions.[79] Therefore, design of host molecules with high affinity and selectivity is of great interest in supramolecular chemistry. The new chiral concave guest[80] with C_3-symmetry (which has a phosphorus atom at the center) showed efficient encapsulation of fullerenes due to cooperative π-π interactions. Josa et al. presented[81] series of buckybowls (with B97-D2/TZVP//SCC-DFTB-D approach) with different size toward designing fullerenes receptors (C_{40}, C_{60}, and C_{70}) via π-π interactions. They concluded from the noncovalent interaction analysis that the shape and rigidity of buckybowls play crucial roles in their ability to interact with fullerenes (Fig. 9). The bowl-shaped hexabenzo-coronene derivative with large size and added flaps showed the interaction energy of ~-50.0 kcal/mol (compound 15 in Fig. 9) as the best receptor candidate for investigated fullerenes. The addition of flaps on the rim of the bowl part of receptor was suggested as the critical factor in designing of receptors.[81]

Moreover, the quintuply charged calix[5]-imidazolium recognizes the neutral C_{60} fullerene in water that could be valuable in aqueous fullerene chemistry. This recognition is confirmed by both theoretical calculations, fluorescence, and NMR spectroscopies.[82] The cavity size of calix[5]imidazolium and the strong π^+-π interaction between positively charged imidazolium ring and aromatic rings of fullerene explain the water solubility of fullerene. The calculated binding energy of calix[5]imidazolium with C_{60} fullerene at B97-D3/TZV2P changes from 21.0 kcal/mol in gas phase to 14.0 kcal/mol in aqueous solution using conductor-like screening model (COSMO).[76]

Recognition of aromatic molecules and nucleobases using π-stacking interactions is of particular interests for researches in DNA sequencing,[83,84] DNA sensing,[85] and drug delivery fields.[86] Graphene is a promising candidate in these applications among other various polycyclic aromatic hydrocarbons because of its sensitivity in interaction with other carbon-based materials.[8,87] The binding energies of Cyt, Thy, Gua, and Ade on graphene (Fig. 10) are predicted to be 18.4, 19.7, 21.7, and 19.8

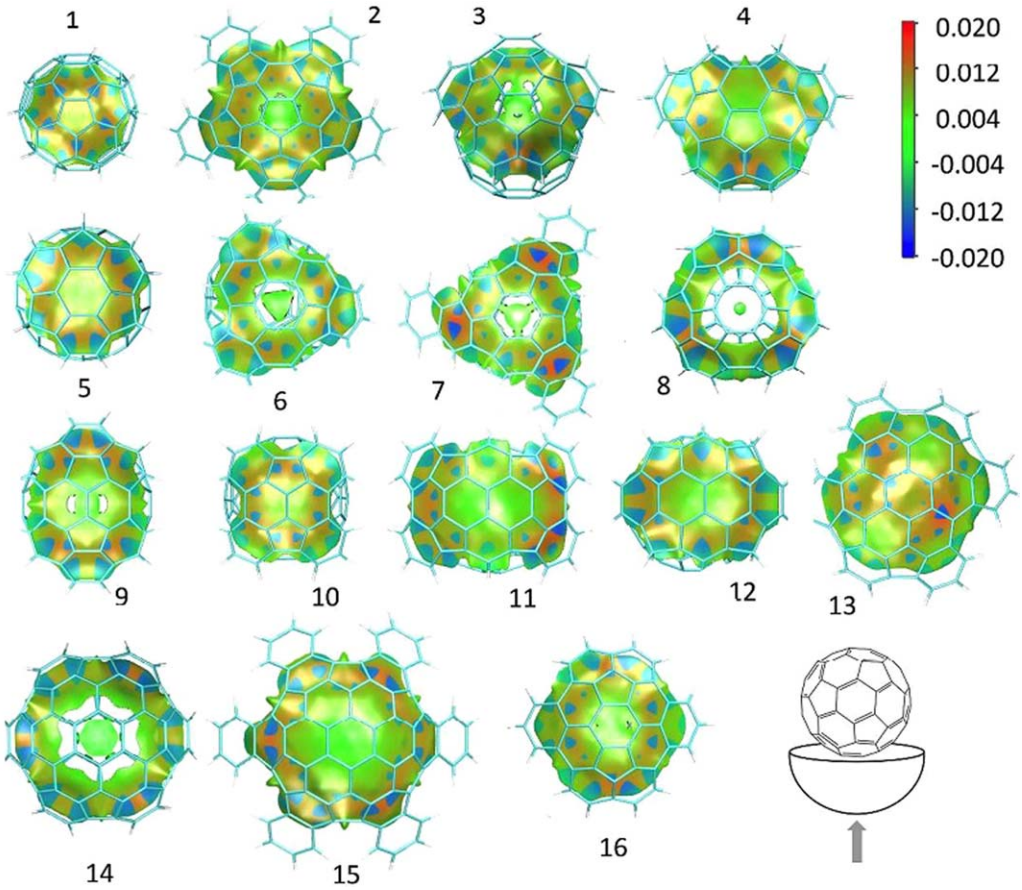

Figure 9. Plot of noncovalent interaction potential gradient isosurface (bottom views with 0.4 a.u.) for fullerenes and receptor models. Blue, green, and red regions indicate strong attractive, weak vdW and strong non-bonded overlap interactions. Reproduced from Ref. [81], with permission from The Royal Society of Chemistry.

kcal/mol at the PBE + TS level.[88] Boron nitride (BN) sheet is also a good alternative to graphene. The hexagonal BN sheet is an insulator (with ~5–7 eV energy gap) with polar nature bond compared with gapless and semimetal graphene with nonpolar carbon-carbon bonds. The binding energies of four types of nucleobase on the BN sheet (Gua > Ade > Thy > Cyt obtained at PBE + vdW) with those on graphene.[89]

To detect each nucleobase in the single-stranded (SS) DNA by means of π-π interaction, a fluidic nanochannel functionalized graphene nanoribbon (GNR) was theoretically designed (Fig. 10).[2] The GNR forms a bridge across nanochannel and controls the orientational fluctuation of individual nucleobases with strong π-π interactions between GNR surface and nucleobases. The strength of π-π interaction controls holding of nucleobases on graphene and translocation of ss-DNA over GNR in the channel.

When a nucleobase stacks on GNR, the ballistic electron transport channel of the GNR which matches with the molecular orbital energy diminishes via Fano resonance so that the ss-DNA strand can be sequenced.[83] The Stark effect of the molecular orbitals of nucleobases can be further exploited for better differentiation between different nucleobases based on 2D molecular electronics spectroscopy (2D-MES) which utilizes the gate voltage scanning on varying bias voltages.[84]

Umadevi and Sastry[86] presented that the binding energy of a carbon nanotube (CNT) with DNA/RNA nucleobase is controlled by the CNT curvature. The π-π-stacking interaction of nucleobases on the surface of CNTs showed the order of Gua > Thy $\approx$ Ade > Cyt > Ura which is in good agreement with experimental results. The maximum binding energies of the nucleobases are observed on graphene surface because the increase in curvature of the surface leads to decrease in interaction energy of the absorbed substrate (Fig. 11).[90] They also mentioned that the interaction energy of aromatic amino acids such as Phe, Tyr, Trp, and His (at the M06-2X/6-311G**//ONIOM level) on the surfaces of carbon nanostructures is controlled by interplay between π-π stacking and CH-π interactions which is stronger in planar graphene than curved CNTs.[90]

Sensors based on noncovalent π-interactions recognize anions via three modes of interactions: (1) σ-interaction with partially positively-charged CH or NH of arenes (C-H$^+$···X$^-$ and N-H$^+$···X$^-$), (2) anion-π interaction between anion and arenes with large, positive quadrupole moment (Q_{zz}),[21] and (3) C-H hydrogen bond with carbon atom of electron-deficient arene (Lewis acidic aromatic rings).[67,91] The σ/π-anion interactions can be significantly enhanced by increasing the magnitude of electron deficiency in arene.

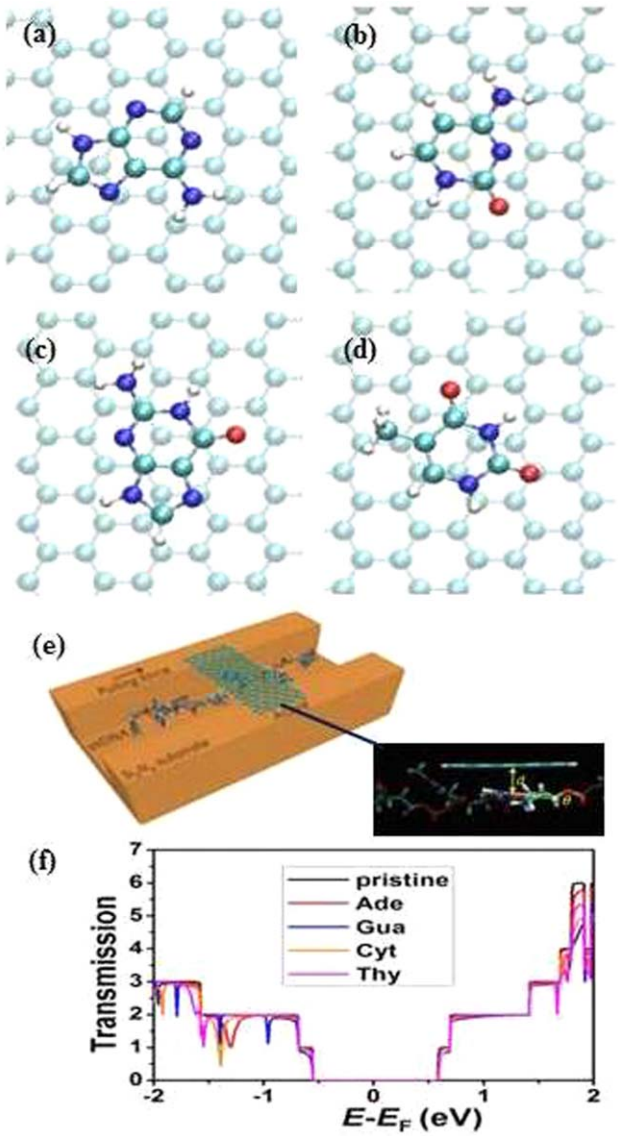

Figure 10. Structures of nucleobases on graphene: a) Gua, b) Ade, c) Thy, d) Cyt;[89] e) schematic of GNR nanochannel design for DNA sequencing and snapshot from a π-π interaction simulation in nanochannel device, where *d*, stacking distance; θ, tilt angle; f) transmission (in G_0) with respect to energy E-E_F (E_F: Fermi energy) of the GNR device with DNA bases stacked, which show strong Fano resonance at the molecular orbital energies of each nucleobase.[5] Reproduced from Refs. [83] and [88], with permission from Nature Publishing Group and American Chemical Society, respectively).

Therefore, electron deficient arenes can be used as neutral receptors for polyanions. The *N*,*N*-naphthalenediimide (NDI) as π-acidic molecule (with electron deficiency region at the center) has a highly positive quadrupole moment (Q_{zz} = +19.4 B; Fig. 10a).[92] Gorteau et al.[92] designed and synthesized oligo-(para-phenylene)-*N*,*N*-naphthalenedi-imide (O-NDI) rods which act as transmembrane anion-π slides with an unusual ion selectivity sequence ($Cl^- > F^- > Br^- > I^-$) for application in cystic fibrosis and other anion channelopathies. The π-anion interactions between electron deficient regions of NDI building units and anions in lipid bilayers (Fig. 12b) cause ion selectivity for the ion transport in this synthetic channel.

The pincer-like, benzene-bridged, fluorescence sensor was designed and synthesized for selective detection of Adenosine-5′-triphosphate (ATP) among various nucleoside triphosphates (CTP, UTP, TTP, and GTP).[93] The sensing mechanism was based on anion-induced changes in fluorescence with a pyrene excimer and imidazolium moieties that serve as fluorescence signal source and phosphate anion receptors, respectively (Fig. 13).

At the COSMO/B97-D/TZV2P level, the most stable structure of this sensor (**1-4Br**$^-$ structure in Fig. 13) exhibits π-π interaction between two pyrene moieties that leads to a strong excimer peak at 487 nm.[93] The **1-ATP-i** complex (i: intercalated; Fig. 13) shows that the phosphate groups of ATP interact with imidazolium moiety via $(C\text{-}H)^+\cdots O^-$ ionic H-bond, and the adenosine of ATP is stacked in between π-rings of pyrene excimer. On the other hand, the pyrimidine moiety of GTP forms the π^+-π interaction in the **1-GTP-o** complex (o: outside the stacked pyrenes; Fig. 13) with positively charged imidazolium ring, and one of the H atom of the imidazole ring in guanine shows CH-π interaction with pyrene ring. Similar binding patterns are expected for CTP, TTP, and UTP due to oxygen atoms present in cytosine, thymine and uracil moieties. Henceforth, the unique sandwich π-π stacking of **1-ATP-i** between pyrene rings causes high selectivity among other nucleoside triphosphates of the sensor. This sensor could be used for ATP-relevant biological processes.[93]

Molecular assembly and crystal engineering

Combination of various noncovalent π interactions can be used for designing new material architecture in solid-state. For instance, the H-bonding interactions and π^+-π/π-π interactions facilitate crystal packing of doubly protonated **MPTPH2** (MPTP = 4′-(4-methoxyphenyl)-2,2′:6′,2″-terpyridine) which used as receptor for halide ions (Cl^- and Br^-) and water molecules.[94]

The **PTPH$_3$** (triply protonated form of 4′-(4-pyridyl)-2,2′:6′,2″-terpyridine, Fig. 14a) has three π^+ moieties (**1A**, **1B,** and **3** pyridinium ring) and neutral π^+ pyridine moiety (ring **2**).[15] Interaction of NO_3^- anions with π^+ systems (via π^+...anion

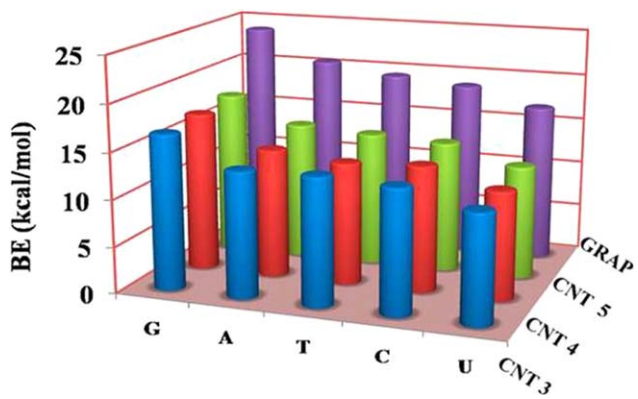

Figure 11. Binding energies (BE in kcal/mol) of CNT (CNT (3,3), CNT(4,4), and CNT(5,5)) and graphene (GRAP) with nucleobases obtained at B3LYP-D/6-31G*//ONIOM. Reproduced from Ref. [86], with permission from American Chemical Society.

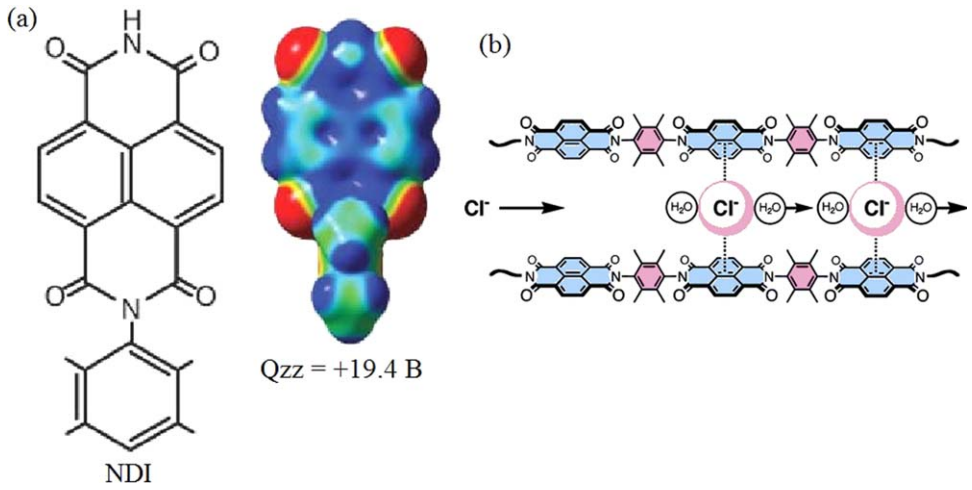

Figure 12. DFT-ESP map of the *N*,*N*-naphthalenediimide unit (NDI) a), oligo-(para-phenylene)-*N*,*N*-naphthalene-diimide (O-NDI) rod as a chloride p-slide in lipid bilayer membranes b). Reproduced from Ref. [92], with permission from American Chemical Society.

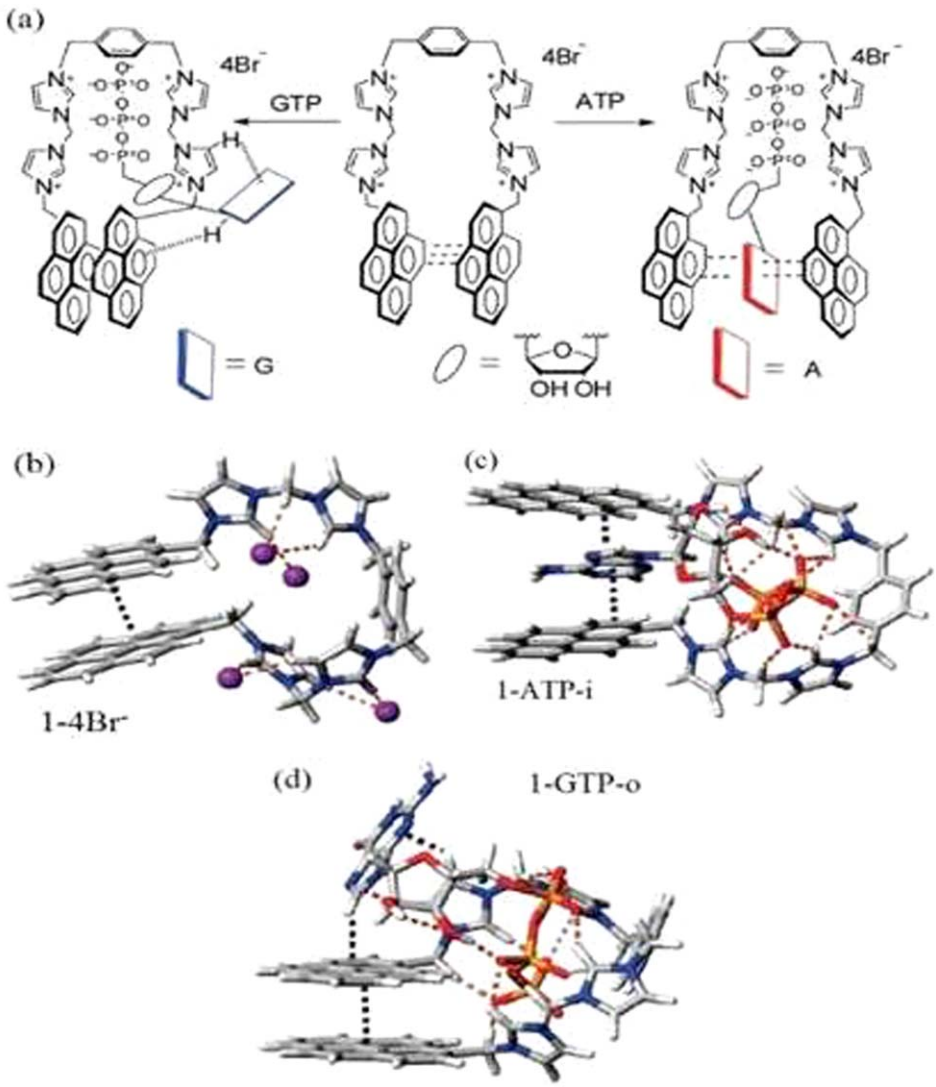

Figure 13. Proposed binding model of the sensor to ATP and GTP a), calculated most stable structure of the sensor b) and its binding modes toward ATP c), and GTP d). CH. . .O^-/OH. . .O hydrogen bonds and CH-π/π-π interactions are denoted by orange and black dotted lines, respectively. Reproduced from Ref. [93], with permission from American Chemical Society.

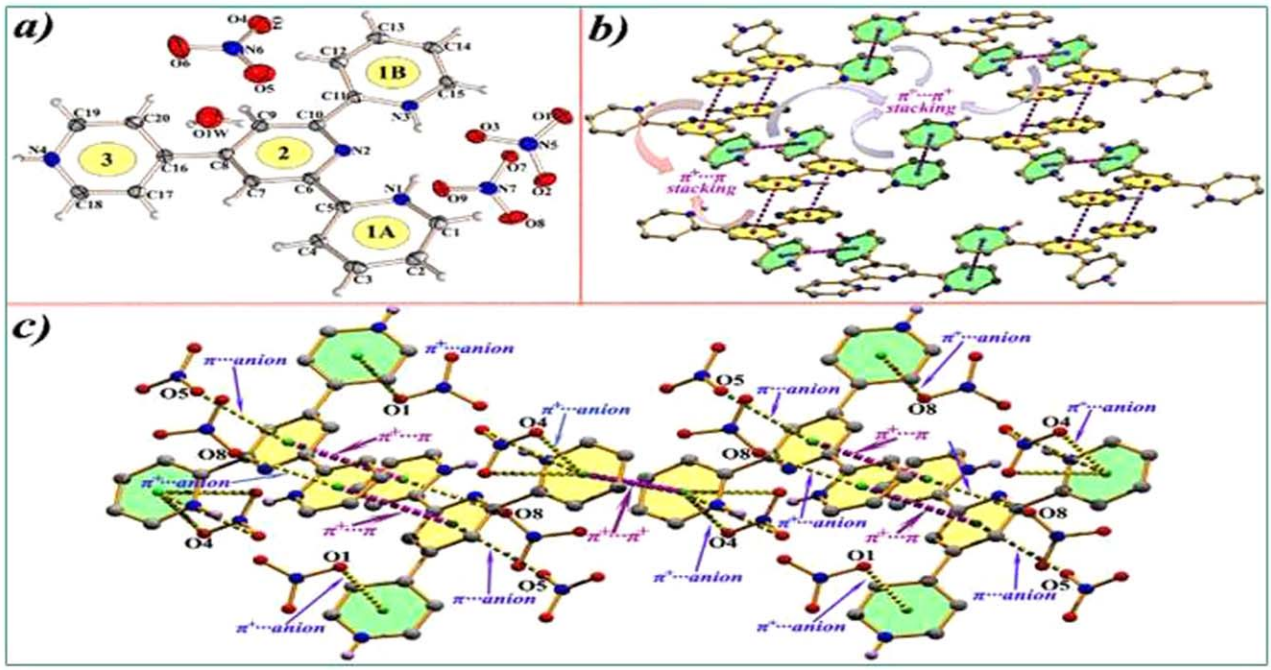

Figure 14. a) $PTPH_3{\cdot}3(NO_3)$ molecule: Rings **1A**, **1B,** and **3** are aromatic cations (π^+), while Ring **2** is neutral (π); stacking arrangement of $PTPH_3$ molecules b) through π^+-π^+ and π^+-π interactions c) through π^+-π^+, π^+-π, π^+-anion, π-anion interactions. Reproduced from Ref. [15], with permission from The Royal Society of Chemistry.

interaction) allows π^+-π^+ interactions as the main driving force of crystal packing in $PTPH_3{\cdot}3(NO_3)$, which is confirmed with both DFT-D (B97-D/TZV2P) calculation and X-ray crystallographic analysis.

Schneebeli et al.[95] designed and synthesized singly right/left handed self-assemble helices of chiral triangular NDI-Δ redox prisms (macrocycle composed of linking three electron-deficient naphthalene diimides together using 1,2-diaminocyclohexane) with I_3^- anion by using cooperative effects of space orbital interaction, π-π/anion-π interactions and electron transfer effects. Watanabe et al.[96] designed novel approach for preparing luminescence helically π-stacked assembly of cationic chiral poly(para-phenylene) derivatives by using cooperative intermolecular electrostatic and π-π interactions. Hourani et al. designed an organic field-effect transistor (OFET) composed of regioregular octamer of 3-hexyl-thiophene $(3HT)_8$ showing anisotropic charge transport properties.[97] In the π-π stacking direction of this polymeric semiconductor (along the long axis of the single crystal with mobility of 10^{-3} $cm^2\ V^{-1}\ s^{-1}$) the charge transport is smaller than that along the molecular axis (in the direction of the thickness of the single crystal with mobility of 0.5 $cm^2\ V^{-1}\ s^{-1}$). Therefore, the π-π stacking interaction controls charge carrier mobility in these polymeric semiconductors.

Molecular catalysts and enzymes

The catalytic role of intra molecular and intermolecular anion-π, π-π, and H-π interactions, and van der Waals interactions in enzyme-inhibitor complexes, drug-receptor interaction, and organocatalyst is less documented.[98] Most of aromatic amino acids such as phenylalanine, tyrosine, tryptophan, and histidine participate in H-π and π-π interactions in proteins and enzymes. The Figure 15 shows the histogram of geometrical parameter (relative orientation of aromatic rings) for π-stacking and T-shaped π-π interactions in proteins.[98]

For example, Lucas et al. reported that T-shaped π-π interaction between benzoxazinone molecule, as novel acetyl lysine mimics for BET bromodomain inhibitor and tryptophan, play important role in selectivity and the recognition site of the target.[99] Pecsi et al.[100] studied the mechanism of phosphate ester hydrolysis in dUTPase by using crystallographic, optical spectroscopy, kinetics, and thermodynamics methods. They found that the aromatic π-π interaction between dUTPase enzyme and nucleotide accelerates rate of enzymatic reaction

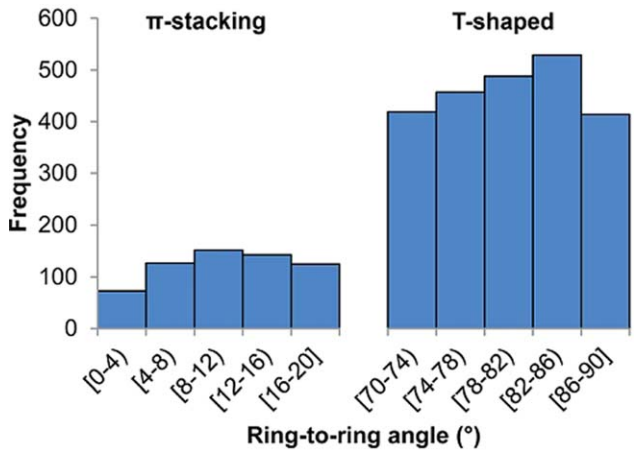

Figure 15. Histogram of ring-to-ring angle distribution for proteins with π-π interactions. Reproduced from Ref. [98], with permission from The Royal Society of Chemistry.

by the stabilization of the transition state of the nucleotide hydrolysis reaction. The oxidative dehydrogenation of polyunsaturated alcohols with molecular oxygen is catalyzed by Aryl-alcohol oxidases (AAO). Ferreira et al.[101] showed that T-shaped stacking interaction between the Tyr92 residue in AAO enzyme and the alcohol substrate is necessary in hydride and proton transfer steps of catalytic reaction. They also investigated the role of electronic character (electron-withdrawing or donating) and number of substituents in alcohol substrates on catalytic activity of AAO using stacking interaction energy calculations and site-directed mutagenesis. Based on their results, the kinetics of the AAO enzymes is governed by the π-π interaction between Tyr92 residue and substrate.[101]

The anion-π interactions between the anionic Asp and Phe54 and Phe116 residues in ketosteroid isomerase enzyme (KSI) and positive electrostatic potential of other aromatic amino acid residues control the active site of this enzyme and facilitate its catalytic activity.[102] The anion-π interaction between Asp92 residue-C12 in human U1A protein and the RNA controls locking/unlocking binding mechanism of this protein to the RNA.[103]

The strength of anion-π interactions could be tuned by using π-acidic aromatic systems with high and positive quadrupole moment. Recently, Zhao et al.[104] developed this idea to design new anion-π interaction organocatalyst which would be widely used in chemical and biological reactions. They used NDI ($Q_{zz} = +19$ B) and its analogues with electron withdrawing substituents with high positive quadrupole moment as strongest π-acid aromatics. They found that model anion-π catalyst stabilizes transition states of enolate intermediates and reactive enolate intermediate (in Michael addition of enones and 1,4-addition reaction with nitroolefins) up to $\Delta\Delta G_{TS} = 11.0$ and $\Delta\Delta G_{RI} = 4.7$ kJ/mol. The experimental and theoretical results[105] on Kemp elimination revealed that transition-state of this reaction is stabilized by anion-π catalyst (i.e., carboxylate base on top of a π-acidic naphthalenediimide) up to up to $\Delta\Delta G_{TS} = 31.8 \pm 0.4$ kJ mol^{-1} which correlates with the π-acidity of catalyst.

Conclusions

The nature and strength of noncovalent π-interactions depend on types of counter interacting molecules with π-system (cation, anion, π, and –CH/NH) and can be tuned and controlled through substituent and heteroatom effects. To achieve this purpose, the SAPT energy decomposition analysis (electrostatic, inductive, dispersive, and exchange repulsive energies), has revealed that dispersion contributions can be quite important in anion-π and π-π interactions. However, though these interactions have widely investigated theoretically, the entropic and solvent effects must be considered in details in computational studies,[105] which will enable theoretical results more practical in experimental applications. Furthermore, some examples of theoretical modeling of molecular and materials design approaches associated with molecular assembly and their nano-bio device applications have been demonstrated in this review. We believe that the state-of-the-art quantum theory aided material design approaches will pave the way toward the development of novel and unique nanomaterials and nanodevices in the coming years.

Keywords: noncovalent interaction · H-π interaction · π-π interaction · anion-π interaction · molecular recognition

How to cite this article: Z. Aliakbar Tehrani, K. S. Kim. *Int. J. Quantum Chem.* **2016**, *116*, 622–633. DOI: 10.1002/qua.25109

[1] R. Sedlak, T. Janowski, M. Pitoňák, J. Řezáč, P. Pulay, P. Hobza, *J. Chem. Theory Comput.* **2013**, *9*, 857.
[2] E. A. Meyer, R. K. Castellano, F. Diederich, *Angew. Chem. Int. Ed.* **2003**, *42*, 1210.
[3] F. J. M. Hoeben, P. Jonkheijm, E. W. Meijer, A. P. H. J. Schenning, *Chem. Rev.* **2005**, *105*, 1491.
[4] J. Singh, H. M. Lee, I. Ch. Hwang, K. S. Kim, *Supramol. Chem.* **2007**, *19*, 321.
[5] P. Tarakeshwar, S. J. Lee, J. Y. Lee, K. S. Kim, *J. Chem. Phys.* **1998**, *108*, 7217.
[6] P. Tarakeshwar, H. S. Choi, K. S. Kim, *J. Am. Chem. Soc.* **2001**, *123*, 3323.
[7] K. S. Kim, P. Tarakeshwar, J. Y. Lee, *Chem. Rev.* **2000**, *100*, 4145.
[8] E. C. Lee, D. Kim, P. JureÄka, P. Tarakeshwar, P. Hobza, K. S. Kim, *J. Phys. Chem. A* **2007**, *111*, 3446.
[9] C. D. Sherrill, *Acc. Chem. Res.* **2013**, *46*, 1020.
[10] N. J. Singh, S. K. Min, D. Y. Kim, K. S. Kim, *J. Chem. Theory Comput.* **2009**, *5*, 515.
[11] I. Geronimo, N. J. Singh, K. S. Kim, *Phys. Chem. Chem. Phys.* **2011**, *13*, 11841.
[12] A. S. Mahadevi, G. N. Sastry, *Chem. Rev.* **2013**, *113*, 2100.
[13] J. Granatier, P. Lazar, M. Otyepka, P. Hobza, *J. Chem. Theory Comput.* **2011**, *7*, 3743.
[14] J. C. Ma, D. A. Dougherty, *Chem. Rev.* **1997**, *97*, 1303.
[15] S. K. Seth, P. Manna, N. J. Singh, M. Mitra, A. D. Jana, A. Das, S. R. Choudhury, T. Kar, S. Mukhopadhyay, K. S. Kim, *Cryst. Eng. Commun.* **2013**, *15*, 1285.
[16] M. Mascal, A. Armstrong, M. D. Bartberger, *J. Am. Chem. Soc.* **2002**, *124*, 6274.
[17] I. Alkorta, I. Rozas, J. Elguero, *J. Am. Chem. Soc.* **2002**, *124*, 8593.
[18] D. Quionero, C. Garau, C. Rotger, A. Frontera, P. Ballester, A. Costa, P. M. Deyà, *Angew. Chem. Int. Ed.* **2002**, *41*, 3389.
[19] D. Kim, P. Tarakeshwar, K. S. Kim, *J. Phys. Chem. A* **2004**, *108*, 1250.
[20] A. Frontera, P. Gamez, M. Mascal, T. J. Mooibroek, J. Reedijk, *Angew. Chem. Int. Ed.* **2011**, *50*, 9564.
[21] P. Gamez, *Inorg. Chem. Front.* **2014**, *1*, 35.
[22] J. N. Tiwari, K. Nath, S. Kumar, R. N. Tiwari, K. C. Kemp, N. H. Le, D. H. Youn, J. S. Lee, K. S. Kim, *Nat. Commun.* **2013**, *4*, 2221.
[23] S. K. Min, Y. Cho, D. R. Mason, J. Lee, K. S. Kim, *J. Phys. Chem. C* **2011**, *115*, 16247.
[24] J. N. Tiwari, K. C. Kemp, K. Nath, R. Tiwari, H. G. Nam, K. S. Kim, *ACS Nano.* **2013**, *7*, 9223.
[25] V. Georgakilas, M. Otyepka, A. B. Bourlinos, V. Chandra, N. Kim, K. C. Kemp, P. Hobza, R. Zboril, K. S. Kim, *Chem. Rev.* **2012**, *112*, 6156.
[26] P. Hobza, H. L. Selzle, E. W. Schlag, *J. Phys. Chem.* **1996**, *100*, 18790.
[27] E. C. Lee, B. H. Hong, J. Y. Lee, J. C. Kim, D. Kim, Y. Kim, P. Tarakeshwar, K. S. Kim, *J. Am. Chem. Soc.* **2005**, *127*, 4530.
[28] M. O. Sinnokrot, C. D. Sherrill, *J. Phys. Chem. A* **2006**, *110*, 10656.
[29] S. Tsuzuki, K. Honda, T. Uchimaru, M. Mikami, K. Tanabe, *J. Am. Chem. Soc.* **2002**, *124*, 104.
[30] R. Podeszwa, R. Bukowski, K. Szalewicz, *J. Phys. Chem. A* **2006**, *110*, 10345.
[31] N. Galand, G. Wipff, *New J. Chem.* **2003**, *27*, 1319.
[32] C. A. Hunter, J. K. M. Sanders, *J. Am. Chem. Soc.* **1990**, *112*, 5525.
[33] S. L. Cockroft, J. Perkins, C. Zonta, H. Adams, S. E. Spey, C. M. R. Low, J. G. Vinter, K. R. Lawson, C. J. Urch, C. A. Hunter, *Org. Biomol. Chem.* **2007**, *5*, 1062.

[34] S. L. Cockroft, C. A. Hunter, K. R. Lawson, J. Perkins, C. Urch, *J. Am. Chem. Soc.* **2005**, *127*, 8594.
[35] I. K. Mati, S. L. Cockroft, *Chem. Soc. Rev.* **2010**, *39*, 4195.
[36] M. O. Sinnokrot, C. D. Sherrill, *J. Phys. Chem. A* **2003**, *107*, 8377.
[37] A. Clements, M. Lewis, *J. Phys. Chem. A* **2006**, *110*, 12705.
[38] S. E. Wheeler, K. N. Houk, *J. Am. Chem. Soc.* **2008**, *130*, 10854.
[39] S. A. Arnstein, C. D. Sherrill, *Phys. Chem. Chem. Phys.* **2008**, *10*, 2646.
[40] S. E. Wheeler, *J. Am. Chem. Soc.* **2011**, *133*, 10262.
[41] J. H. Williams, *Acc. Chem. Res.* **1993**, *26*, 593.
[42] H. R. Marsden, G. E. M. Fraaije, A. Kros, *Angew. Chem. Int. Ed.* **2010**, *49*, 8570.
[43] H. Zheng, J. Gao, *Angew. Chem.* **2010**, *122*, 8817.
[44] K. Szalewicz, *Wiley Interdiscip. Rev.: Comput. Mol. Sci.* **2012**, *2*, 254.
[45] A. Heßelmann, G. Jansen, M. Schutz, *J. Chem. Phys.* **2005**, *122*, 014103.
[46] R. Bukowski, R. Podeszwa, K. Szalewicz, *Chem. Phys. Lett.* **2005**, *414*, 111.
[47] S. Grimme, *WIRES Comput. Mol. Sci.* **2011**, *1*, 211.
[48] S. Grimme, J. Antony, S. Ehrlich, H. Krieg, *J. Chem. Phys.* **2010**, *132*, 154104.
[49] A. Tkatchenko, M. Scheffler, *Phys. Rev. Lett.* **2009**, *102*, 073005.
[50] A. D. Becke, E. R. Johnson, *J. Chem. Phys.* **2007**, *127*, 154108.
[51] M. Dion, H. Rydberg, E. Schröder, D. C. Langreth, B. I. Lundqvist, *Phys. Rev. Lett.* **2004**, *92*, 246401.
[52] Y. Cho, W. J. Cho, I. S. Youn, G. Lee, N. J. Singh, K. S. Kim, *Acc. Chem. Res.* **2014**, *47*, 3321.
[53] K. E. Riley, M. Pitoňák, P. Jurečka, P. Hobza, *Chem. Rev.* **2010**, *110*, 5023.
[54] M. O. Sinnokrot, C. D. Sherrill, *J. Am. Chem. Soc.* **2004**, *126*, 7690.
[55] R. M. Parrish, C. D. Sherrill, *J. Am. Chem. Soc.* **2014**, *136*, 17386.
[56] E. G. Hohenstein, C. D. Sherrill, *J. Phys. Chem. A* **2009**, *113*, 878.
[57] I. Geronimo, E. Ch. Lee, N. J. Singh, K. S. Kim, *J. Chem. Theory Comput.* **2010**, *6*, 1931.
[58] B. L. Schottel, H. T. Chifotides, K. R. Dunbar, *Chem. Soc. Rev.* **2008**, *37*, 68.
[59] O. B. Berryman, V. S. Bryantsev, D. P. Stay, D. W. Johnson, B. P. Hay, *J. Am. Chem. Soc.* **2007**, *129*, 48.
[60] B. P. Hay, R. Custelcean, *Cryst. Growth Des.* **2009**, *9*, 2539.
[61] B. P. Hay, V. S. Bryantsev, *Chem. Commun.* **2008**, 2417.
[62] A. Bauzá, P. M. Deyà, A. Frontera, D. Quiñonero, *Phys. Chem. Chem. Phys.* **2014**, *16*, 1322.
[63] D. Y. Kim, N. J. Singh, K. S. Kim, *J. Chem. Theory Comput.* **2008**, *4*, 1401.
[64] D. Y. Kim, I. Geronimo, N. J. Singh, H. M. Lee, K. S. Kim, *J. Chem. Theory Comput.* **2012**, *8*, 274.
[65] C. Garau, A. Frontera, D. Quinonero, P. Ballester, A. Costa, P. M. Deyà, *ChemPhysChem* **2003**, *4*, 1344.
[66] C. Garau, D. Quinonero, A. Frontera, P. Ballester, A. Costa, P. M. Deyá, *Org. Lett.* **2003**, *5*, 2227.
[67] S. E. Wheeler, K. N. Houk, *J. Phys. Chem. A* **2010**, *114*, 8658.
[68] O. B. Berryman, D. W. Johnson, *Chem. Commun.* **2009**, *22*, 3143.
[69] S. E. Wheeler, J. W. G. Bloom, *Chem. Commun.* **2014**, *50*, 11118.
[70] P. D. Mezei, G. I. Csonka, A. Ruzsinszky, J. Sun, *J. Chem. Theory Comput.* **2015**, *11*, 360.
[71] I. Geronimo, N. J. Singh, K. S. Kim, *J. Chem. Theory Comput.* **2011**, *7*, 825.
[72] A. Quinonero, D. Frontera, P. Escudero, A. Ballester, P. M. Costa, Deyà, *ChemPhysChem* **2007**, *8*, 1182.
[73] C. Garau, D. Quinonero, A. Frontera, P. Ballester, A. Costa, P. M. Deyà, *J. Phys. Chem. A* **2005**, *109*, 9341.
[74] C. Garau, D. Quinonero, A. Frontera, P. Ballester, A. Costa, P. M. Deyà, *New J. Chem.* **2003**, *27*, 211.
[75] D. Kim, E. C. Lee, K. S. Kim, P. Tarakeshwar, *J. Phys. Chem. A* **2007**, *111*, 7980.
[76] A. Frontera, D. Quinonero, A. Costa, P. Ballester, P. M. Deyà, *New J. Chem.* **2007**, *31*, 556.
[77] J. Y. Lee, B. H. Hong, D. Y. Kim, D. R. Mason, J. W. Lee, Y. Chun, K. S. Kim, *Chem. Eur. J.* **2013**, *19*, 9118.
[78] J. Y. Lee, B. H. Hong, W. Y. Kim, S. K. Min, Y. Kim, M. V. Jouravlev, R. Bose, K. S. Kim, I. C. Hwang, L. J. Kaufman, C. W. Wong, P. Kim, K. S. Kim, *Nature* **2009**, *460*, 498.
[79] N. Martin; J.-F. Nierengarten, Supramolecular Chemistry of Fullerenes and Carbon Nanotubes; Wiley-VCH: Weinheim, **2012**.
[80] M. Yamamura, T. Saito, T. Nabeshima, *J. Am. Chem. Soc.* **2014**, *136*, 14299.
[81] D. Josa, I. González-Veloso, J. Rodríguez-Otero, E. M. Cabaleiro-Lago, *Phys. Chem. Chem. Phys.* **2015**, *17*, 6233.
[82] Y. Chun, N. J. Singh, I. C. Hwang, J. W. Lee, S. U. Yu, K. S. Kim, *Nat. Commun.* **2013**, *4*, 1797.
[83] S. K. Min, W. Y. Kim, Y. Cho, K. S. Kim, *Nat. Nanotech.* **2011**, *6*, 162.
[84] A. C. Rajan, M. R. Rezapour, J. Yun, Y. Cho, W. J. Cho, S. K. Min, G. Lee, K. S. Kim, *ACS Nano* **2014**, *8*, 1827.
[85] B. Shirinfar, N. Ahmed, Y. S. Park, G. S. Cho, I. S. Youn, J. K. Han, H. G. Nam, K. S. Kim, *J. Am. Chem. Soc.* **2013**, *135*, 90.
[86] D. Umadevi, G. N. Sastry, *J. Phys. Chem. Lett.* **2011**, *2*, 1572.
[87] S. Thomas, A. C. Rajan, M. R. Rezapour, K. S. Kim, *J. Phys. Chem. C* **2014**, *118*, 10855.
[88] Y. Cho, S. K. Min, J. Yun, W. Y. Kim, A. Tkatchenko, K. S. Kim, *J. Chem. Theory Comput.* **2013**, *9*, 2090.
[89] J. H. Lee, Y. K. Choi, H. J. Kim, R. H. Scheicher, J. H. Cho, *J. Phys. Chem. C* **2013**, *117*, 13435.
[90] D. Umadevi, G. N. Sastry, *ChemPhysChem* **2013**, *14*, 2570.
[91] J. Ran, P. Hobza, *J. Chem. Theory Comput.* **2009**, *5*, 1180.
[92] V. Gorteau, G. Bollot, J. Mareda, A. Perez-Velasco, S. Matile, *J. Am. Chem. Soc.* **2006**, *128*, 14788.
[93] Z. Xu, N. J. Singh, J. Lim, J. Pan, H. N. Kim, S. Park, K. S. Kim, J. Yoon, *J. Am. Chem. Soc.* **2009**, *131*, 15528.
[94] A. Das, A. D. Jana, S. K. Seth, B. Dey, S. R. Choudhury, T. Kar, S. Mukhopadhyay, N. J. Singh, I. C. Hwang, K. S. Kim, *J. Phys. Chem. B* **2010**, *114*, 4166.
[95] S. T. Schneebeli, M. Frasconi, Z. Liu, Y. Wu, D. M. Gardner, N. L. Strutt, C. Cheng, R. Carmieli, M. R. Wasielewski, J. F. Stoddart, *Angew. Chem. Int. Ed.* **2013**, *52*, 13100.
[96] K. Watanabe, Z. Sun, K. Akagi, *Chem. Mater.* **2015**, *27*, 2895.
[97] W. Hourani, K. Rahimi, I. Botiz, F. P. V. Koch, G. Reiter, P. Lienerth, T. H. Heiser, J. Bubendorffa, L. Simon, *Nanoscale* **2014**, *6*, 4774.
[98] X. Lucas, A. Bauzá, A. Fronterab, D. Quiñonero, *Chem. Sci.* **2016**, *7*, 1050.
[99] X. Lucas, D. Wohlwend, M. Hugle, K. Schmidtkunz, S. Gerhardt, R. Schule, M. Jung, O. Einsle, S. Gunther, *Angew. Chem. Int. Ed.* **2013**, *52*, 14055.
[100] I. Pecsi, I. Leveles, V. Harmat, B. G. Vertessy, J. Toth, *Nucleic Acids Res.* **2010**, *38*, 7179.
[101] P. Ferreira, A. Hernandez-Ortega, F. Lucas, J. Carro, B. Herguedas, K. W. Borrelli, V. Guallar, A. T. Martınez, M. Medina, *FEBS J.* **2015**, *282*, 3091.
[102] J. P. Schwans, F. Sunden, J. K. Lassila, A. Gonzalez, Y. Tsai, D. Herschlag, *Proc Natl Acad Sci USA* **2013**, *110*, 1308.
[103] M. Blech, D. Peter, P. Fischer, M. M. T. Bauer, M. Hafner, M. Zeeb, H. Nar, *J. Mol. Biol.* **2013**, *425*, 94.
[104] Y. Zhao, N. Sakai, S. Matile, *Nat. Commun.* **2014**, *5*, 3911.
[105] D. Y. Kim, N. J. Singh, J. W. Lee, K. S. Kim, *J. Chem. Theory Comput* **2008**, *4*, 1162.

Received: 30 September 2015
Revised: 9 December 2015
Accepted: 21 January 2016
Published online 18 February 2016